Cell Reports, Volume *26*

Supplemental Information

Cortical State Fluctuations across Layers of V1 during Visual Spatial Perception

Anderson Speed, Joseph Del Rosario, Christopher P. Burgess, and Bilal Haider

SUPPLEMENTARY FIGURES

Figure S1

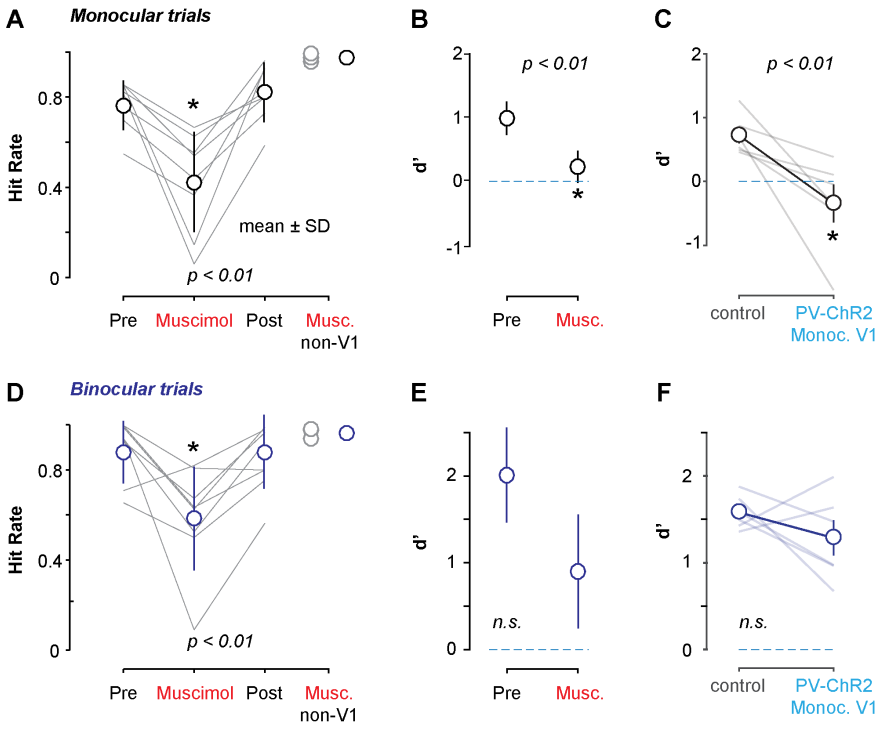

Fig. S1. Inactivation of monocular V1 selectively impairs monocular visual detection (related to Fig.1).

A. Intracortical injection of muscimol into monocular V1 significantly impaired monocular detection (Hit rates: 76% ± 11% versus 42 ± 22%; mean ± SD; $p < 0.01$ Wilcoxon signed-rank test). Hit rates recovered the next day (82 ± 11%). Inactivation of adjacent cortex (retrosplenial or parietal) did not affect hit rates, nor did injection of artificial cerebrospinal fluid in V1 (not shown). Injection sites were mapped for spatial selectivity before inactivation (Fig. S3). See Methods for inactivation protocol.

B. Inactivation significantly reduced monocular detection sensitivity (d'; 0.97 ± 0.3 vs. 0.21 ± 0.3; mean ± SD); $p < 0.01$ Wilcoxon signed-rank test). Sensitivity during inactivation is not significantly different from chancel level ($p = 0.3$, sign test).

C. Optogenetic inhibition of monocular V1 (interleaved on 25% of trials) significantly reduced monocular d' (0.72 ± 0.13 to -0.34 ± 0.3; mean ± SD; $p < 0.05$; Wilcoxon signed-rank test; n = 6 days and 1500 trials). Data from one PV-cre x A1-32-ChR2 mouse.

D-E. Same sessions as **A-B**, muscimol inactivation significantly reduced binocular hit rates (88 ± 14% versus 59 ± 23%, $p < 0.01$, Wilcoxon signed-rank test), but did not significantly reduce sensitivity compared to control conditions (d'; 2.0 ± 0.5 vs. 0.9 ± 0.7; $p = 0.1$, Wilcoxon signed-rank test), and d' remained significantly above chance levels ($p < 0.01$, sign test).

F. Same sessions as **C,** optogenetic inhibition had no significant effect on binocular detection (d': 1.58 ± 0.08 to 1.29 ± 0.2; $p = 0.69$).

Figure S2

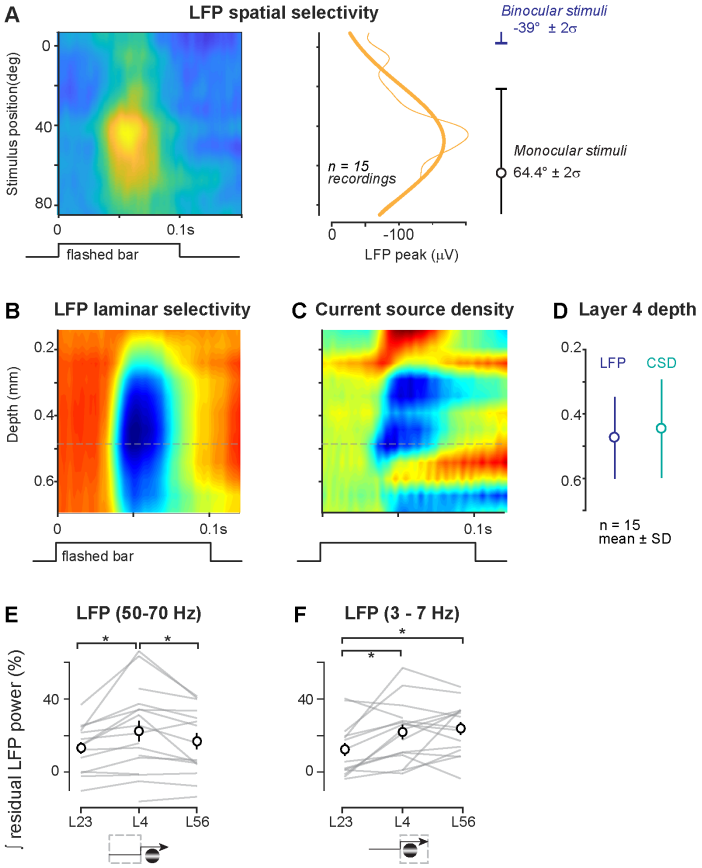

Fig. S2. Spatial tuning and laminar analysis of LFP residual power (related to Fig. 2).

A. Left**,** average space-time receptive field (RF) maps of local field potential (LFP) responses across the population (n = 15 recordings). Right, peak LFP responses (thin line) and Gaussian fit (thick line). LFP responses peak at 44 ± 52˚ (mean ± 2σ of fit), monocular stimulus presented at 64 ± 30˚ (mean ± 2σ of Gabor). Note that the Binocular stimulus was nearly 100˚ away.

B. Example recording of average laminar LFP response to high contrast bars flashed at the center of the receptive field. Dashed line indicates depth of maximum LFP response. 32 sites spanning 775 microns. Data interpolated and smoothed for display, see Methods.

C. Current source density (CSD) calculated for recording in A. Earliest and largest current sink corresponds to the site of maximum LFP response (dashed line, as in A).

D. Estimated Layer 4 depth from LFP peak (466 ± 123 μm, blue) versus CSD sink (453 ± 154 μm, teal). We defined L4 to span ± 100 microns around the location of the CSD sink within recordings. Both depth estimates agree with prior functional and anatomical localization of L4 in mouse V1 (Lien and Scanziani, 2013; Pluta et al., 2015).

E. Pre-stimulus narrowband gamma (50 – 70 Hz) residual power across layers. All electrode contacts within a layer were averaged within individual experiments (lines), then averaged across experiments (black, mean ± SEM, n = 17). A few recordings used electrodes that did not span all layers. Residual narrowband gamma power in L4 (0.22 ± 0.06) significantly greater than L2/3 (0.13 ± 0.03; $p < 0.001$) and L5/6 (0.17 ± 0.04; $p < 0.01$). L2/3 and L5/6 not significantly different ($p = 0.09$; one-tailed paired signed rank tests for all).

F. Stimulus-evoked low frequency (3 – 7 Hz) residual power across layers. Same experiments as A. L4 residual power (0.22 ± 0.04) significantly greater than L2/3 (0.12 ± 0.04; $p < 0.01$). L4 and L5/6 (0.24 ± 0.04) not significantly different ($p = 0.68$). L5/6 significantly greater than L2/3 ($p = 0.01$; one-tailed paired signed rank tests for all).

Figure S3

Figure S3. Pre-stimulus activity of fast spiking (FS) and regular spiking (RS) neurons during visual spatial detection (related to Fig. 3).

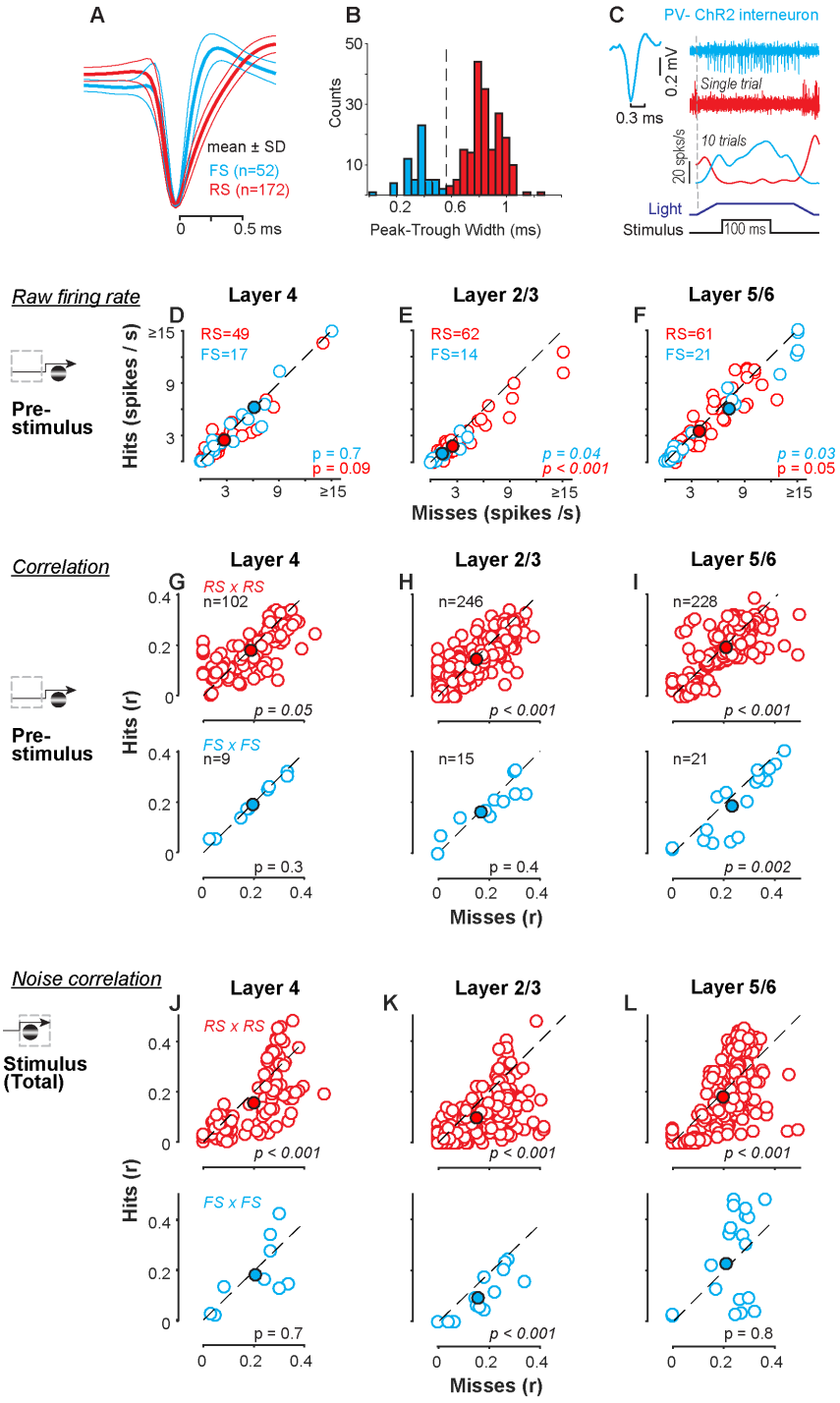

A-B. Mean waveforms of RS (red, n = 172) and FS (cyan, n = 52) neurons (± SD), and histogram of all peak to trough spike widths.

C. PV interneuron spikes directly activated by photostimulation of channelrhodopsin (bottom). PV spike width (0.3 ms) overlaps with mode of FS neurons in B.

D-F. Pre-stimulus firing rates before detection failure (Miss trials, abscissa) versus success (Hit trials, ordinate). Layers identified with current source density (see Fig. S2). Regular spiking (RS) units fired less before Hits versus Misses, in all layers (L4: 2.5 ± 0.8 vs. 2.7 ± 0.8 spikes / s; L2/3: 1.8 ± 0.3 vs. 2.4 ± 0.5; L5/6: 3.5 ± 0.5 vs. 3.8 ± 0.5; mean ± SEM), and significantly less in L2/3 ($p < 0.001$, Wilcoxon paired signed-rank test). FS neurons also fired significantly less before Hit trials in L2/3 and L5/6 (L2/3: 1.0 ± 0.3 vs. 1.3 ± 0.4 spikes / s; L5/6: 6.1 ± 1.6 vs. 7.3 ± 2.0 spikes / s; $p < 0.05$, Wilcoxon signed-rank test for both), but not in L4 (L4: 6.2 ± 2.2 vs. 6.1 ± 2.0; $p = 0.7$). Spikes counted from stimulus onset to reaction time (Hits), or until stimulus offset (Misses).

G-I. Total correlations before stimulus onset in RS neuron pairs (Top, RS x RS, red) and FS neuron pairs (Bottom, FS x FS, cyan) within layers. RS pairs were significantly less correlated prior to Hits versus Misses in L2/3 and L5/6 (L2/3: 0.14 ± 0.006 vs. 0.15 ± 0.007; L5/6: 0.19 ± 0.006 vs. 0.21 ± 0.007; mean ± SEM; $p < 0.01$, Wilcoxon signed-rank test for all), with similar trends in L4 (L4: 0.179 ± 0.008 vs. 0.188 ± 0.01; $p = 0.05$). FS pairs significantly reduced noise correlations L5/6 before Hit trials (L5/6: 0.19 ± 0.03 vs. 0.23 ± 0.03; $p < 0.05$), but not L4 or L2/3 (L4: 0.19 ± 0.03 vs. 0.19 ± 0.04; $p = 0.2$; L2/3: 0.19 ± 0.03 vs. 0.23 ± 0.03; $p < 0.01$).

J-L. Noise correlations during stimulus in RS neuron pairs (Top, RS x RS, red) and FS neuron pairs (Bottom, FS x FS, cyan) within layers. RS pairs were significantly less correlated prior to Hits, in all layers (L4: 0.15 ± 0.01 vs. 0.20 ± 0.01; L2/3: 0.10 ± 0.006 vs. 0.15 ± 0.007; L5/6: 0.18 ± 0.009 vs. 0.20 ± 0.007; mean ± SEM; $p < 0.001$, Wilcoxon signed-rank test for all). FS pairs significantly reduced noise correlations before successful detection in L2/3 (L2/3: 0.09 ± 0.02 vs. 0.15 ± 0.03; $p < 0.001$), but not L4 or L5/6 (L4: 0.18 ± 0.05 vs. 0.20 ± 0.04; $p = 0.7$; L5/6: 0.23 ± 0.04 vs. 0.21 ± 0.03; $p = 0.8$).

Figure S4

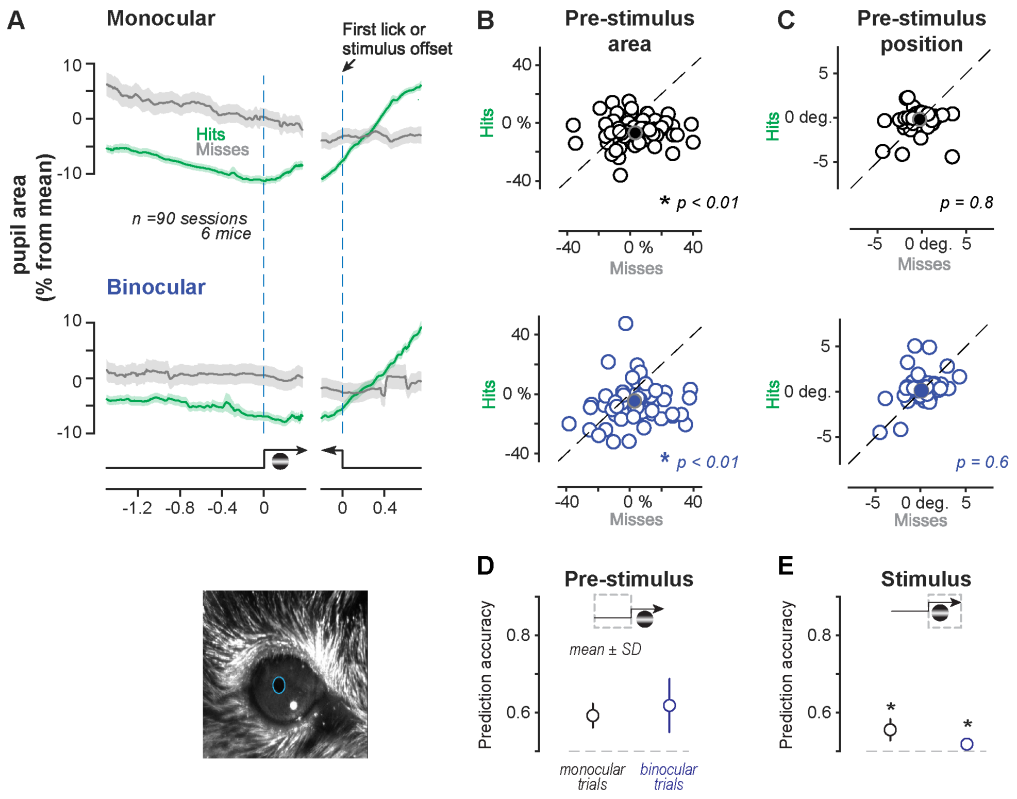

Figure S4. Pupil dynamics and single-trial predictions of visual spatial detection (related to Fig. 4)

A. Pupil area (Δ% from mean of entire session) before successful detection (Hits, green) of monocular (top rows) and binocular stimuli (bottom rows). Pupil dilates rapidly after the first lick and reward consumption on all Hit trials. Monocular grating stimulated the imaged eye. Same experiments during interleaved blocks of trials. Mean ± SEM, 90 sessions in 6 mice.

B. Pupil area was significantly smaller before Hits in both monocular (top, 4 ± 13%; mean ± SD; $p < 0.01$) and binocular trials (bottom, 3 ± 16%; $p < 0.01$ for both, Wilcoxon signed-rank test).

C. Pre-stimulus pupil position was not significantly different before Hits versus Misses in either monocular (0.5 ± 2.3˚ versus -0.5 ± 2.3˚; mean ± SD; $p = 0.8$) or binocular trials (-0.1 ± 2.3˚, -0.1 ± 2.6˚; $p = 0.6$,Wilcoxon signed-rank test).

D. Pre-stimulus pupil area predicted single trial detection of monocular (60 ± 3% accuracy; mean ± SD) and binocular (62 ± 7%) stimuli significantly better than chance (dashed line; $p < 0.01$, sign test for both). Pre-stimulus predictions were slightly but significantly better on binocular versus monocular trials ($p = 0.02$; rank sum test).

E. Pupil area was significantly less predictive during the stimulus (monocular: 56 ± 3%; binocular: 52 ± 1%; $p < 0.001$ rank sum tests; pre-stimulus versus stimulus, within location). Moreover, during the stimulus, predictions were superior for monocular versus binocular detection ($p < 0.001$, rank sum test).

Figure S5

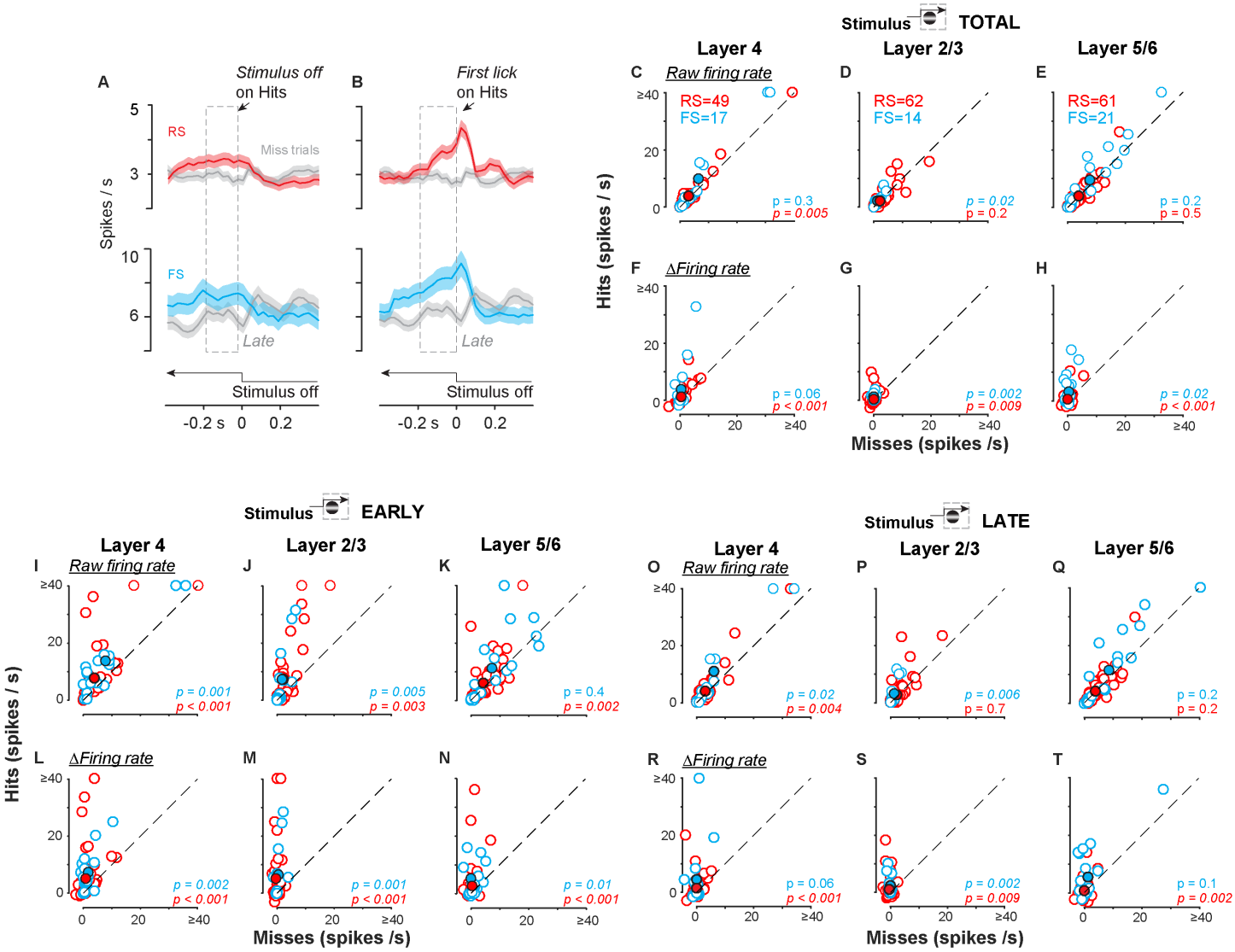

Figure S5. Stimulus-evoked firing rates of RS and FS neurons during visual spatial detection (related to Fig.3)

A-B. Comparison of late stimulus activity, (A) aligned to stimulus offset on Hits, or (B) aligned to first lick on hits for RS (red, top) and FS (cyan, bottom) neurons. Late stimulus activity ramps up to first lick and then abruptly returns to baseline during reward consumption.

C-E. Firing rates during the entire stimulus period for detection failure (Miss trials, abscissa) versus success (Hit trials, ordinate). Layers identified with current source density (see Fig. S2). Regular spiking (RS) units fired significantly more during Hits versus Misses in L4 (L4: 3.8 ± 1.1 versus 3.2 ± 0.9 spikes / s; mean ± SEM; $p < 0.01$, Wilcoxon signed-rank test), but not in L2/3 or L5/6 (L2/3: 2.3 ± 0.4 versus 2.3 ± 0.4; L5/6: 4.1 ± 0.6 versus 3.9 ± 0.5 spikes / s; $p = 0.2$ and $p = 0.5$). FS neurons fired significantly more during Hits versus Misses in L2/3 (L2/3: 2.1 ± 0.6 versus 1.4 ± 0.4 spikes / s; $p = 0.02$, Wilcoxon signed-rank test), but not in L4 or L5/6 (L4: 10.1 ± 4.2 versus 6.5 ± 2.3 spikes / s; L5/6: 9.4 ± 2.5 versus 7.5 ± 2.0 spikes / s; $p = 0.3$ and $p = 0.2$). Spikes counted from stimulus onset to reaction time (Hits), or until stimulus offset (Misses).

F-H. Same as C-E, for stimulus evoked firing rate relative to pre-stimulus baseline (ΔFiring rate). RS units in all layers showed significantly greater ΔFiring rate on Hit versus Miss trials (L4: 1.3 ± 0.4 versus 0.5 ± 0.3 spikes / s; L2/3: 0.4 ± 0.3 versus -0.1 ± 0.2; L5/6: 0.6 ± 0.2 versus 0.1 ± 0.1 spikes / s; $p < 0.01$ for all, Wilcoxon signed-rank test). FS units in L2/3 and L5/6 showed significantly greater ΔFiring rate on Hit trials (L2/3: 1.1 ± 0.3 versus 0.1 ± 0.1; L5/6: 3.3 ± 1.1 versus 0.2 ± 0.2 spikes / s; $p < 0.01$ for all, Wilcoxon signed-rank test), but not in L4 (L4: 3.8 ± 2.1 versus 0.4 ± 0.4 spikes / s; $p = 0.06$).

I-K. Same as C-E, for firing rates during the early stimulus period (0 – 0.2s after stimulus onset; Fig. 3A). RS units fired significantly more during the early stimulus period on Hits versus Misses, across all layers (L4: 7.9 ± 2.1 versus 3.7 ± 1.0 spikes / s; L2/3: 7.2 ± 2.5 versus 2.3 ± 0.4; L5/6: 6.1 ± 1.0 versus 4.1 ± 0.5 spikes / s; $p < 0.01$ for all, Wilcoxon signed-rank test). FS neurons also fired significantly more during the early stimulus period on Hits versus Misses in L4 and L2/3 (L4: 13.8 ± 3.7 versus 7.6 ± 2.6 spikes / s; L2/3: 7.4 ± 2.8 versus 1.8 ± 0.6 spikes / s; $p < 0.01$ for both, Wilcoxon signed-rank test), but not in L5/6 (L5/6: 11.4 ± 3.4 versus 7.2 ± 1.8 spikes / s; $p = 0.4$).

L-N. Same as I-K, for evoked firing rate during Early stimulus period, relative to pre-stimulus baseline (∆Firing rate). RS units in all layers showed significantly greater ∆Firing rate on Hit versus Miss trials (L4: 5.4± 1.8 versus 1.0 ± 0.4 spikes / s; L2/3: 5.3 ± 2.4 versus -0.1 ± 0.2; L5/6: 2.6 ± 0.8 versus 0.3 ± 0.2 spikes / s; $p < 0.001$ for all, Wilcoxon signed-rank test). Same for FS units in all layers (L4: 7.5 ± 1.7 versus 1.6 ± 0.7 spikes / s; L2/3: 6.4 ± 2.6 versus 0.4 ± 0.3; L5/6: 5.3 ± 2.0 versus -0.1 ± 1.0 spikes / s; $p \leq 0.01$ for all, Wilcoxon signed-rank test).

O-Q. Same as G-I, for firing rates during the Late stimulus period (-0.2s to first lick for Hits, or stimulus offset for Misses). RS units fired significantly more during the late stimulus period on Hits versus Misses in L4 (L4: 4.0 ± 1.3 versus 2.8 ± 0.8 spikes / s; $p < 0.01$, Wilcoxon signed-rank test), but not in L2/3 or L5/6 (L2/3: 2.7 ± 0.6 versus 2.1 ± 0.4; L5/6: 4.2 ± 0.7 versus 3.8 ± 0.5 spikes / s; $p = 0.7$ and $p = 0.2$). FS neurons also fired significantly more during the Late stimulus period on Hits versus Misses in L4 and L2/3 (L4: 10.9 ± 4.6 versus 6.0 ± 2.3 spikes / s; L2/3: 3.3 ± 1.1 versus 1.1 ± 0.3 spikes / s; $p = 0.02$ and $p < 0.01$, Wilcoxon signed-rank test), but not in L5/6 (L5/6: 11.6 ± 3.4 versus 8.6 ± 2.9 spikes / s; $p = 0.2$).

R-T. Same as M-O, for change in evoked firing rate during Late stimulus period, relative to pre-stimulus baseline (∆Firing rate). RS units in all layers showed significantly greater ∆Firing rate on Hit versus Miss trials (L4: 1.5 ± 0.5 versus 0.1 ± 0.2 spikes / s; L2/3: 0.8 ± 0.4 versus -0.4 ± 0.2; L5/6: 0.7 ± 0.3 versus 0.01 ± 0.1 spikes / s; $p < 0.01$ for all, Wilcoxon signed-rank test). FS units fired significantly more during the Late stimulus period on Hits versus Misses in L2/3 (L2/3: 2.3 ± 0.8 versus -0.2 ± 0.1; $p \leq 0.01$ for all, Wilcoxon signed-rank test), but not other layers (L4: 4.6 ± 2.5 versus -0.05 ± 0.5 spikes / s; L5/6: 5.4 ± 2.0 versus 1.3 ± 1.3 spikes / s; $p = 0.06$ and $p = 0.1$).

Figure S6

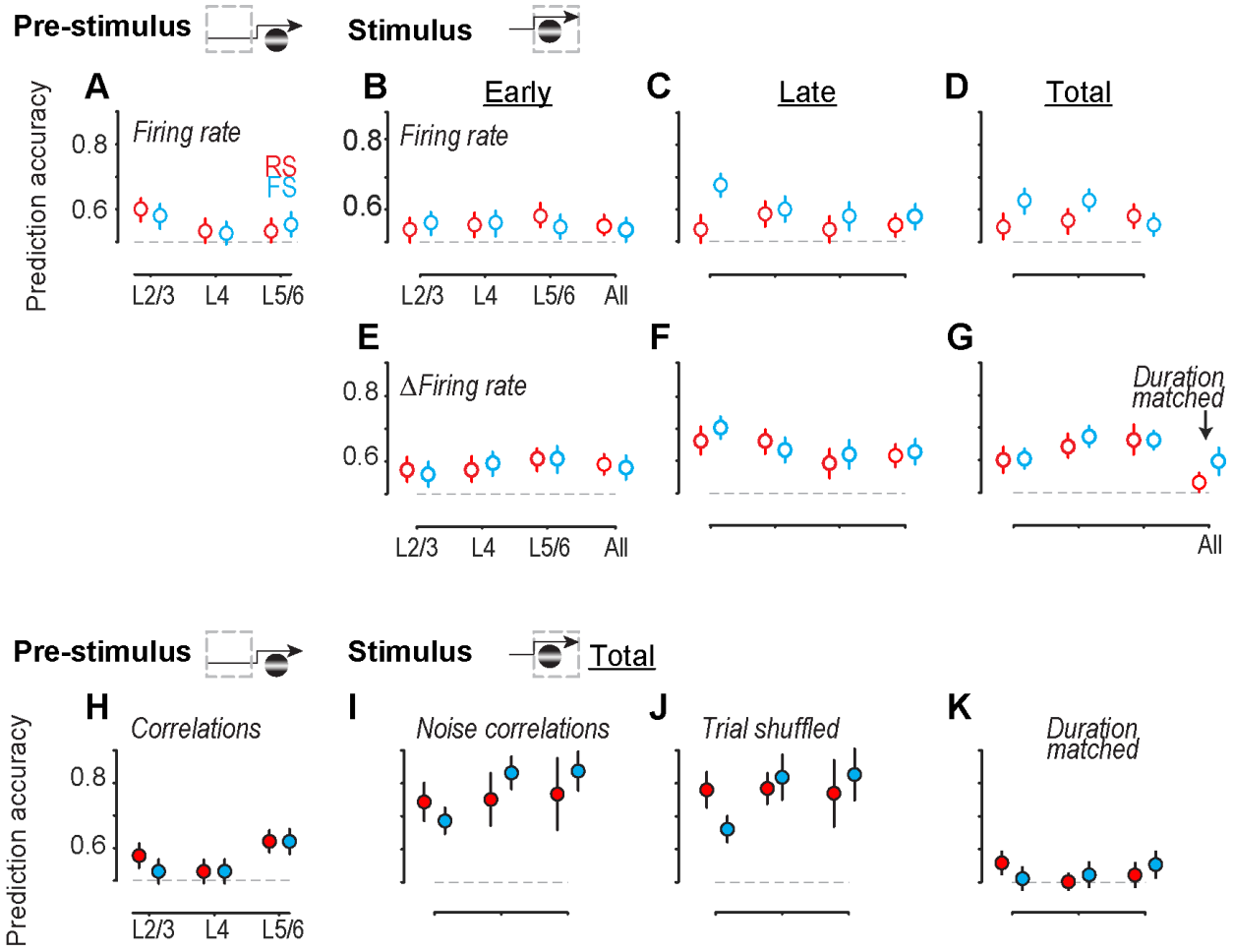

Figure S6. Stimulus-evoked activity of RS and FS neurons during visual spatial detection (related to Fig.4)

A. Single-trial prediction accuracy of behavioral outcome from regular spiking (RS) and fast spiking (FS) neuron firing rates preceding stimulus onset in L2/3 (RS, 0.60 ± 0.04; FS, 0.58 ± 0.04, mean ± SD), L4 (RS, 0.53 ± 0.04; FS, 0.53 ± 0.04), and L5/6 (RS, 0.54 ± 0.04; FS, 0.55 ± 0.04). RS cells in L2/3 were significantly better than both FS and RS cells in L4 and L5/6. FS cells in L2/3 predicted significantly better than FS cells in L4 ($p < 0.01$, Kruskal-Wallis, multiple comparisons).

B. Prediction accuracy from evoked firing rate during Early sensory response. L2/3 (RS, 0.54 ± 0.04; FS, 0.56 ± 0.04, mean ± SD), L4 (RS, 0.55 ± 0.04; FS, 0.56 ± 0.04), L5/6 (RS, 0.58 ± 0.04; FS, 0.55 ± 0.04), and sampled across all layers (RS, 0.55 ± 0.04; FS, 0.54 ± 0.04). L5/6 RS cells predicted significantly better than L2/3 RS cells ($p < 0.01$, Kruskal-Wallis, multiple comparisons).

C. Prediction accuracy from evoked firing rate during Late sensory response. L2/3 (RS, 0.54 ± 0.04; FS, 0.68 ± 0.04, mean ± SD), L4 (RS, 0.59 ± 0.04; FS, 0.6 ± 0.04), and L5/6 (RS, 0.54 ± 0.04; FS, 0.58 ± 0.04) and sampled across all layers (RS, 0.55 ± 0.04; FS, 0.58 ± 0.04). L2/3 FS cells were significantly better than all other cells, L4 FS and RS cells predicted significantly better than L2/3 and L5/6 RS cells ($p < 0.01$, Kruskal-Wallis, multiple comparisons).

D. Prediction accuracy from evoked firing rate during Total sensory response. L2/3 (RS, 0.55 ± 0.04; FS, 0.63 ± 0.04, mean ± SD), L4 (RS, 0.56 ± 0.04; FS, 0.63 ± 0.04), and L5/6 (RS, 0.58 ± 0.04; FS, 0.55 ± 0.03) and sampled across all layers (RS, 0.55 ± 0.04; FS, 0.55 ± 0.04). L2/3 and L4 FS cells predicted significantly better than all other cells ($p < 0.01$, Kruskal-Wallis, multiple comparisons).

E. As in B, for evoked firing rate relative to pre-stimulus baseline (∆Firing rate), during Early stimulus period. L2/3 (RS, 0.58 ± 0.04; FS, 0.56 ± 0.04, mean ± SD), L4 (RS, 0.58 ± 0.04; FS, 0.60 ± 0.04), and L5/6 (RS, 0.60 ± 0.04; FS, 0.61 ± 0.04) and sampled across all layers (RS, 0.59 ± 0.04; FS, 0.58 ± 0.04). L5/6 FS and RS predicted better than L2/3 FS ($p < 0.01$, Kruskal-Wallis, multiple comparisons).

F. As in C, for evoked firing rate relative to pre-stimulus baseline (∆Firing rate), during Late stimulus period. L2/3 (RS, 0.66 ± 0.04; FS, 0.70 ± 0.04, mean ± SD), L4 (RS, 0.66 ± 0.04; FS, 0.63 ± 0.04), and L5/6 (RS, 0.60 ± 0.05; FS, 0.62 ± 0.04) and sampled across all layers (RS, 0.62 ± 0.03; FS, 0.62 ± 0.04). L2/3 FS were better than L5/6 FS and RS. L2/3 and L4 RS predicted behavior better than L5/6 RS ($p < 0.01$, Kruskal-Wallis, multiple comparisons).

G. As in D, for evoked firing rate relative to pre-stimulus baseline (∆Firing rate), during Total stimulus period. L2/3 (RS, 0.60 ± 0.04; FS, 0.60 ± 0.03, mean ± SD), L4 (RS, 0.65 ± 0.04; FS, 0.67 ± 0.03), and L5/6 (RS, 0.66 ± 0.05; FS, 0.66 ± 0.03) and sampled across all layers (RS, 0.62 ± 0.04; FS, 0.63 ± 0.03), and sampled across all layers with Miss trial durations truncated at the average reaction time for Hits (RS, 0.54 ± 0.04; FS, 0.60 ± 0.03). L4 FS and L5/6 FS and RS predicted better than L2/3 FS and RS ($p < 0.01$, Kruskal-Wallis, multiple comparisons). Duration Matched RS prediction accuracy was not significantly better than chance.

H. Prediction accuracy from pairwise (total) correlations between regular spiking (RSxRS, red) and fast spiking (FSxFS, cyan) neurons preceding stimulus onset in L2/3 (RSxRS, 0.58 ± 0.04; FSxFS, 0.53 ± 0.04), L4 (RSxRS, 0.53 ± 0.04; FSxFS, 0.53 ± 0.04), and L5/6 (RSxRS, 0.62 ± 0.03; FSxFS, 0.62 ± 0.04). L5/6 FSxFS and RSxRS correlations predicted better than L2/3 FSxFS and RSxRS, and L4 RSxRS ($p < 0.01$, Kruskal-Wallis, multiple comparisons).

I. Prediction accuracy from noise correlations (see Methods), during Total stimulus period in L2/3 (RSxRS, 0.74 ± 0.06; FSxFS, 0.69 ± 0.04), L4 (RSxRS, 0.75 ± 0.09; FSxFS, 0.83 ± 0.05), and L5/6 (RSxRS, 0.77 ± 0.11; FSxFS, 0.84 ± 0.06). L4 FSxFS predicted better than L2/3FSxFS and RSxRS, while L5/6FSxFS predicted better than L2/3 FSxFS, and better than L2/3 and L4 RSxRS ($p < 0.01$, Kruskal-Wallis, multiple comparisons).

J. Prediction accuracy from trial-shuffled noise correlations, during Total stimulus period in L2/3 (RSxRS, 0.77 ± 0.06; FSxFS, 0.65 ± 0.04), L4 (RSxRS, 0.78 ± 0.05; FSxFS, 0.81 ± 0.07), and L5/6 (RSxRS, 0.76 ± 0.1; FSxFS, 0.83 ± 0.09). L4 and L5/6 FSxFS predicted better than L2/3 FSxFS ($p < 0.01$, Kruskal-Wallis, multiple comparisons).

K. Prediction accuracy from noise correlations, with Miss trial durations truncated at the average reaction time for Hits in L2/3 (RSxRS, 0.56 ± 0.04; FSxFS, 0.51 ± 0.04), L4 (RSxRS, 0.50 ± 0.03; FSxFS, 0.52 ± 0.04), and L5/6 (RSxRS, 0.52 ± 0.04; FSxFS, 0.55 ± 0.04). L2/3 FSxFS and L4 RSxRS predictions were not significantly better than chance.

Figure S7

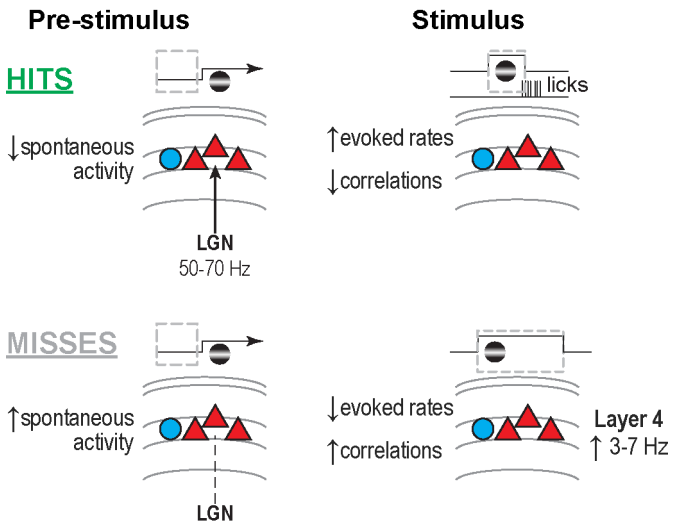

Figure S7. Summary of cortical state changes during visual perceptual behavior (related to Fig. 4)

Top, Hit trials are preceded by low spontaneous activity and strong 50-70 Hz narrowband gamma from LGN. Visual stimuli evoke higher firing rates and lower noise correlations during correct detection.

Bottom, Miss trials are preceded by high spontaneous activity and weak coupling with LGN. Visual stimuli evoke lower firing rates, higher noise correlations, and strong 3-7 Hz oscillations in Layer 4 during detection failures.